Chinese Chemical Letters 36 (2025) 110215

Contents lists available at ScienceDirect

Chinese Chemical Letters

journal homepage: www.elsevier.com/locate/cclet

Emerging sulfide-polymer composite solid electrolyte membranes

Xingjie Li[a,1], Chengjun Yi[a,1], Weifei Hu[a], Huishan Zhang[a], Jiale Xia[a,*], Yuanyuan Li[b,*], Jinping Liu[a,*]

[a] School of Chemistry, Chemical Engineering and Life Science, State Key Laboratory of Advanced Technology for Materials Synthesis and Processing, Wuhan University of Technology, Wuhan 430070, China
[b] School of Integrated Circuits, Huazhong University of Science and Technology, Wuhan 430074, China

ARTICLE INFO

Article history:
Received 4 June 2024
Revised 17 June 2024
Accepted 4 July 2024
Available online 4 July 2024

Keywords:
All-solid-state lithium batteries
Sulfide solid electrolyte
Composite electrolyte
Membrane processing
High energy density

ABSTRACT

Sulfide solid electrolytes with an ultrahigh ionic conductivity are considered to be extremely promising alternatives to liquid electrolytes for next-generation lithium batteries. However, it is difficult to obtain a thin solid electrolyte layer with good mechanical properties due to the weak binding ability between their powder particles, which seriously limits the actual energy density of sulfide all-solid-state lithium batteries (ASSLBs). Fortunately, the preparation of sulfide-polymer composite solid electrolyte (SPCSE) membranes by introducing polymer effectively reduces the thickness of solid electrolytes and guarantees high mechanical properties. In this review, recent progress of SPCSE membranes for ASSLBs is summarized. The classification of components in SPCSE membranes is first introduced briefly. Then, the preparation methods of SPCSE membranes are categorized according to process characteristics, in which the challenges of different methods and their corresponding solutions are carefully reviewed. The energy densities of the full battery composed of SPCSE membranes are further given whenever available to help understanding the device-level performance. Finally, we discuss the potential challenges and research opportunities for SPCSE membranes to guide the future development of high-performance sulfide ASSLBs.

1. Introduction

Lithium-ion batteries (LIBs) have been extensively used in portable electronic devices, even electric vehicles and grid-scale energy storage, due to their high energy densities and long cycle life. However, conventional LIBs based on flammable and leakable liquid electrolytes have serious safety concerns [1-3]. Substituting potentially unsafe liquid electrolytes with non-flammable solid-state electrolytes has the potential to fundamentally resolve the mentioned issue. Furthermore, mechanically rigid solid-state electrolytes can effectively inhibit the dendrite growth when coupled with Li metal anode that has a high specific capacity (3860 mAh/g) and low potential (−3.04 V *vs.* the standard hydrogen electrode (SHE)), which is expected to further enhance the energy density for meeting the ever-increasing demands [4-6]. Consequently, solid electrolytes have attracted significant attention and been developed rapidly for all-solid-state lithium batteries (ASSLBs), making substantial progress in both theoretical research and commercial applications [7-9].

Solid-state electrolytes can be primarily classified into polymer solid electrolytes, oxide solid electrolytes, and sulfide solid electrolytes based on their compositions. Polymer solid electrolytes, typically consisting of polymers and Li salts, have been widely studied for their favorable film-forming properties and low cost, but their ionic conductivities are relatively low, especially at room temperature (10^{-7}–10^{-4} S/cm) [10-12]. Fortunately, both oxides solid electrolytes and sulfides solid electrolytes have high ionic conductivity [13]; for instance, the ionic conductivities of sulfide solid electrolytes can even exceed 10^{-3} S/cm. Moreover, sulfide solid electrolytes also deliver other notable advantages, such as excellent mechanical ductility and effective interfacial contact capability. These attributes position sulfide solid electrolytes highly promising for commercial applications. Although powders of sulfide solid electrolytes can be directly cold pressed into membranes because of their high compressibility and susceptibility to plastic deformation, the mechanical performances of the sulfide thin films are poor, which is basically caused by weak bonding strength between powders [14-16].

To prevent the sulfide solid electrolytes membrane from being punctured and causing a short circuit in the battery, the thick-

* Corresponding authors.
E-mail addresses: jialexia@whut.edu.cn (J. Xia), liyynano@hust.edu.cn (Y. Li), liujp@whut.edu.cn (J. Liu).
[1] These authors contributed equally to this work.

https://doi.org/10.1016/j.cclet.2024.110215
1001-8417/

ness of most sulfide solid electrolytes was designed to exceed 500 μm, much more than that of commercial separators in liquid LIBs [17-21]. This significantly diminishes the actual energy density of ASSLBs based on sulfide solid electrolytes, losing the high energy benefit they offer. Thus, it is crucial to prepare thin films of sulfide solid electrolytes with good mechanical properties. Currently, pulse laser deposition and vapor-phase deposition have been demonstrated as effective methods for preparing thin-film sulfide solid electrolytes [22,23]. However, the cost of these manufacture methods is high and the techniques are generally difficult to scale up. Advanced sulfide solid electrolytes should feature not only the high ionic conductivity, elevated thermal stability, exceptional mechanical properties, but also low manufacturing costs, straightforward and scalable preparation technologies. Alternatively, incorporating polymers as binders or toughened supporting structures in inorganic rigid sulfide solid electrolytes creates sulfide-polymer composite solid electrolyte (SPCSE) membranes with high mechanical strength, continuous ion-conducting networks and good interfacial contact with electrode. This method is regarded as a pragmatic approach for improving mechanical properties while scaling up production [24-26]. Although there have been several reviews about the preparation processes of SPCSE membranes, the challenges faced by different processes have not been well analyzed in a categorized manner, and the summary of the energy densities of ASSLB devices using SPCSE membranes as well as the existing challenges in boosting the energy density has never been considered yet.

In this review, we present a systematic overview of fabrication processes of SPCSE membranes reported in recent years. This review begins with the classification of sulfide and polymer components in composite electrolytes. Based on this categorization, the preparation processes of SPCSE membranes will be divided into three categories, including slurry coating, dry binder laminating and skeleton templating. The merits and demerits of all three strategies are discussed in detail, especially effective solutions to the challenges are presented. Additionally, the energy densities of the full cells of ASSLBs using SPCSE membranes have also been collected whenever available. At the end, possible perspectives concerning future development are presented.

2. General roles and classification of constituents in SPCSE membranes

The SPCSE membranes mainly consist of sulfide solid electrolytes and polymer, where the sulfide solid electrolytes provide ionic conductivity as the main component and the polymer is used to improve the bonding ability between the electrolytes powders to ensure the integrity of the SPCSE membrane. Sulfide solid electrolytes originate from oxide solid electrolytes, where sulfur replaces oxygen in their composition. Sulfide solid electrolytes, based on their crystal structures, are commonly classified into glass, glass-ceramic, Li-argyrodite, thio-Li super ionic conductor (LISICON), and $Li_{10}GeP_2S_{12}$ (LGPS) type [27]. In recent years, sulfide solid electrolytes have gained rapid development, among these, some species of sulfide solid electrolytes exhibit ion conductivity comparable to commercially available organic electrolytes. This, to some extent, has greatly promoted the development and application of sulfide solid electrolytes. For instance, Kato *et al*. reported that $Li_{9.54}Si_{1.74}P_{1.44}S_{11.7}Cl_{0.3}$ even has an ion conductivity as high as 25 mS/cm at room temperature [28].

Polymer plays a crucial role in influencing the physical and chemical properties of SPCSE membranes. From the function of the polymer in the SPCSE membrane, it can be divided into polymer binders and polymer toughened supporting structures [29,30]. Polymer binders are used in nearly all production processes. Since most polymer binders are ionic insulators and excess binders can hinder ion conduction between powders of sulfide solid electrolytes. Choosing and designing highly adhesive binders can decrease their proportion in SPCSE membranes, thus minimizing the ion-blocking effects of binders. Utilizing ion-conductive polymer binders is another strategy to reduce hindering effects. Ion-conductive polymer solid electrolyte materials are frequently used for designing composite membranes, such as polyethylene oxide (PEO)-$LiClO_4$ [31], polyvinylidene difluoride (PVDF)-lithium bis(trifluoromethanesulfonyl)imide (LiTFSI) [32], and nitrile-butadiene rubber (NBR)-LiTFSI [33]. These materials not only behave good compatibility with sulfide solid electrolytes, but also, with the introduction of lithium salts, enhance the transport of lithium ions between sulfide solid electrolytes powders. However, the ion transport efficiency of these polymers, while aiding in Li^+ transport, is significantly lower compared to sulfide solid electrolytes. Generally, the ion conductivity of SPCSE membranes is lower than that of the sulfide solid electrolytes powders themselves. In wet processing techniques, the introduction of organic solvents results in the degradation of sulfide solid electrolytes, thereby further diminishing their intrinsic ion conductivity [34]. Additionally, to further enhance the mechanical strength of the aforementioned processes, polymer toughened supporting structures are additionally added in the skeleton templating method.

The ion conductivity of sulfide solid electrolytes is generally estimated using the following Eq. 1:

$$\sigma = l/RS \tag{1}$$

where l represents the thickness of the electrolyte membrane, R is the resistance, and S is the effective surface area of the electrolyte membrane. Since the ionic conductivity of different types of sulfide solid electrolytes reported in the existing literature varies greatly, relying solely on the ion conductivity of composite membranes is inadequate to reflect the functionalization effect of polymer binders and other factors during the preparation process. Consequently, we propose the term of the ion conductivity retention rate (σ_m/σ_p) as a pivotal indicator factor. Represented in tables of this review, this factor signifies the ratio of ion conductivity of SPCSE membranes (σ_m) to that of powdered solid electrolytes (σ_p). The attained value is crucial for assessing the preparation techniques of SPCSE membranes and understanding the roles of constituents.

3. Strategies toward SPCSE membranes

Presently, the preparation processes for SPCSE membranes can be broadly classified into three methods (Fig. 1): (1) Slurry coating method. Specifically, the sulfide solid electrolytes and polymer binder are well dispersed in a solution, then the mixture is cast onto a substrate (such as a polytetrafluoroethylene film (PTFE)) using the casting method, and the solvent is evaporated to yield a SPCSE membrane. This method is straightforward, compatible with existing production equipment, and suitable for large-scale manufacturing. (2) Dry binder laminating method. The key to this method is to prepare SPCSE membranes by blending sulfide solid electrolytes with polymer binders using a roll-to-roll hot or cold pressing techniques. This solvent-free dry process is environmentally friendly and maximizes the inherent advantages of the high ion conductivity of sulfide solid electrolytes. (3) Skeleton templating method. This method can be briefly described as the embedding of sulfide solid electrolytes with a continuous ion pathway through solution casting or pressure-assisted infiltration into an existing supporting structure. SPCSE membranes prepared using this method exhibit superior mechanical properties, significantly simplifying the assembly difficulty of batteries. Moreover,

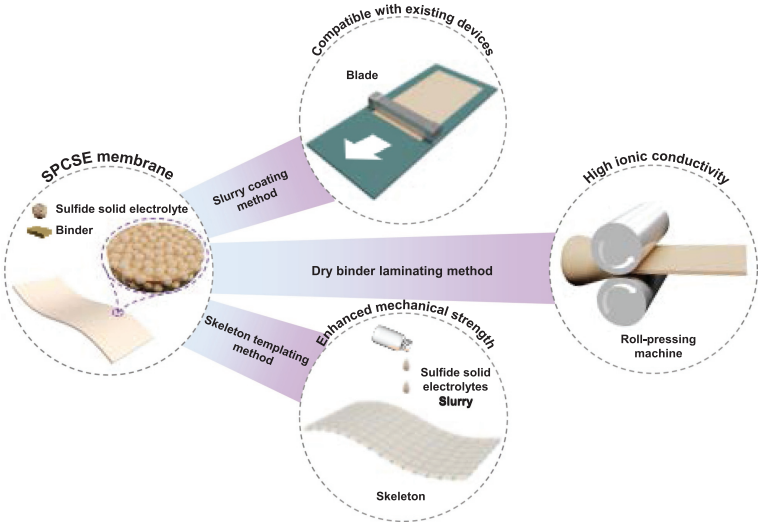

Fig. 1. Schematic of preparation processes of three kinds of SPCSE membranes.

this approach holds the potential for better compatibility with high-capacity and large-volume deformation electrode materials.

3.1. Slurry coating method

In this method, the sulfide electrolyte powder and polymer binder are homogenized in a solvent to form the electrolyte slurry, which is subsequently coated on a substrate material with a scraper, and the SPCSE membrane can be eventually obtained through drying, compaction and other steps. Using this strategy, the controllable solid electrolyte thickness is generally realized by changing the thickness range of the scraper and the calendering pressure. This method is simple, efficient, cost-effective, and compatible with wet electrode manufacturing equipment, rendering it suitable for the large-scale production of SPCSE membranes.

Unfortunately, commonly used binder-solvent systems, including PVDF in *N*-methyl-2-pyrrolidone (NMP), poly(vinylidene fluoride-*co*-hexafluoropropylene) (PVDF-HFP) in dimethylformamide (DMF), and carboxymethylcellulose sodium (CMC) in water, are unsuitable for fabricating SPCSE membranes. Traditional binders, containing polar functional groups, often necessitate strongly polar solvents for dissolution. High-polarity solvents, functioning as strong Lewis bases, frequently incorporate highly electronegative elements like N and O. These elements can readily participate in nucleophilic reactions with sulfides [34]. Furthermore, sulfur atoms in sulfide thio-phosphate ions ($P_2S_7^{4-}$ and PS_4^{3-}) may react with the electrophilic carbon atoms in solvents, resulting in the formation of low ionic conductivity phases and, consequently, reducing the overall ionic conductivity. While low-polarity solvents would decrease the solubility of the binder, affecting the preparation and performances of SPCSE membranes.

Therefore, finding an appropriate solvent-binder system becomes crucial to strike a balance and optimize the performances of the SPCSE membrane. Tan *et al.* explored the effects of common solvents on sulfide solid electrolytes [35]. They used water, methyl ethyl ketone (MEK), tetrahydrofuran (THF), NMP, DMF, acetonitrile (ACN), dimethyl carbonate (DMC), toluene (TOL), and xylene (XYL) as a solvent to disperse the $Li_7P_3S_{11}$ separately, while observing color changes in all solutions. In water, NMP, and DMF solutions, a deep green and blue color emerged, indicating a severe reaction between sulfide solid electrolytes and the solvents. Sulfide solid electrolytes precipitated with a yellow color in MEK, THF, and ACN, indicating self-degradation (Fig. 2a). The precipitates were collected for X-ray diffraction (XRD) characterization, which revealing that XRD patterns of the solute in ACN and DMC no longer match the $Li_7P_3S_{11}$ crystal structure, whereas the solute in TOL and XYL remains essentially unchanged from the original image (Fig. 2b). In the electrochemical impedance spectroscopy (EIS) spectra of sulfide solid electrolytes after solvent removal (Fig. 2c), sulfide solid electrolytes in ACN and DMC show more decomposition by-products, leading to a larger charge transfer resistance.

Yamamoto *et al.* have put forward more explicit guidelines for solvent selection [36], suggesting a donor number less than or equal to 9 with an appropriate vapor pressure. Solvents with donor numbers exceeding 14 exhibit strong electron-donating abilities, rendering them susceptible to nucleophilic attack and subsequent decomposition of sulfide solid electrolytes, resulting in reduced ionic conductivity. Simultaneously, an appropriate vapor pressure can prevent the formation of cracks and protrusions during the drying process (Fig. 2d).

Besides choosing appropriate solvents, the tolerance of sulfide solid electrolytes to solvents can be enhanced through doping modifications [37]. Recently, Zhao *et al.* achieved excellent toluene resistance and lithium stability in sulfide solid electrolytes by doping $SbCl_3$ into LGPS, yielding $Li_{9.88}GeP_{1.96}Sb_{0.04}S_{11.88}Cl_{0.12}$ (Fig. 2e). The partial substitution of P with a smaller, electronegative Sb to form SbS_4^{3-}, which has a lowed adsorption energy and reactivity with toluene molecules, contributing to enhanced tolerance. Moreover, Cl doping aids in forming a LiCl passivation layer on the surface of Li negative electrode, enhancing interface stability. Employing poly(methyl methacrylate/*n*–butyl acrylate) (p(MMA/nBA)) as a binder and TOL as a solvent, they fabricated a SPCSE membrane with an ionic conductivity of 1.9×10^{-3} S/cm (Fig. 2f). With a thickness of 8 μm, this film represents one of the thinnest SPCSE membranes reported to date (Fig. 2g). Their work offers new insights into addressing the compatibility challenges between sulfide solid electrolytes and solvents.

Polymer binders play a crucial role in determining the excellent performances of SPCSE membranes. An appropriate quantity of binder ensures a tight binding of sulfide solid electrolytes powders, guaranteeing a continuous ion-conducting network and binding capability between powders, while an excess of ion-insulating binder can impede grain boundary transport between sulfide solid electrolytes powders, further affecting the powder conductivity of the SPCSE membranes. Researchers currently employ the following strategies to address the aforementioned challenges: (1) Using polymer binders with Li^+ conductivity to mitigate ion-insulating properties through the introduction of lithium salts. (2) Design of

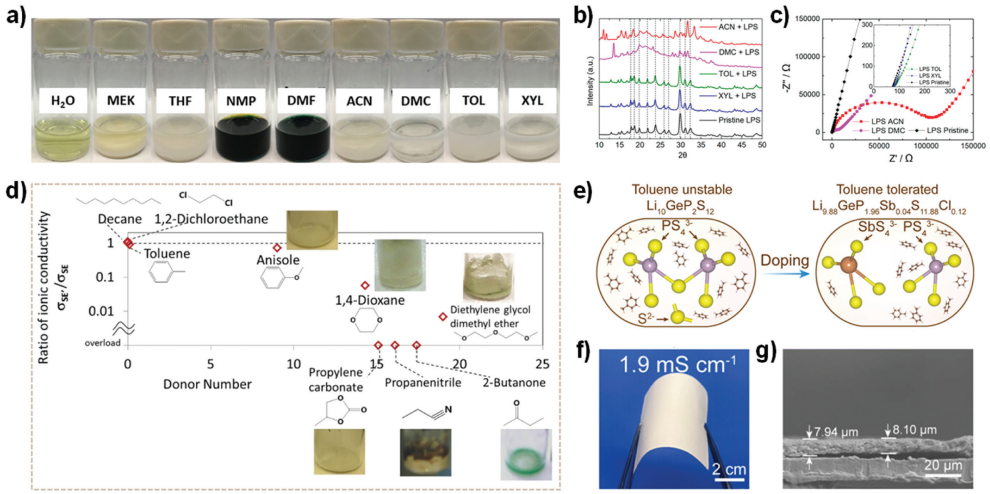

Fig. 2. (a) $Li_7P_3S_{11}$ changes color in different solvents. The $Li_7P_3S_{11}$ after solvent removal compared with the original $Li_7P_3S_{11}$ of (b) XRD patterns and (c) Nyquist plots. Copied with permission [35]. Copyright 2017, American Chemical Society. (d) The influence function of different solvent providers on the ionic conductivity of $75Li_2S{\cdot}25P_2S_5$. (e) Schematic diagram of improving toluene resistant sulfide electrolyte by doping modification. Copied with permission [36]. Copyright 2018, Nature. The SPCSE membrane of (f) optical photo and (g) cross-sectional morphologies. Copied with permission [37]. Copyright 2022, American Chemical Society.

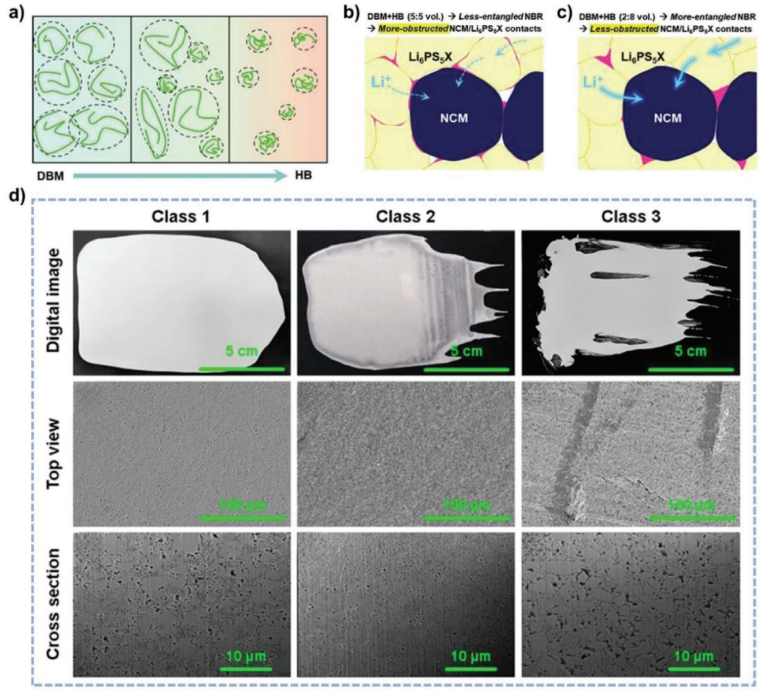

Fig. 3. (a) Schematic diagram of chain segments of NBR polymer in DBM and HB cosolvents with different composition ratios. Effect of DBM and HB on electrode microstructure at volume ratios of (b) 5:5 and (c) 2:8. Copied with permission [33]. Copyright 2021, Wiley. (d) Optical and SEM images of three typical SPCSE membranes. Copied with permission [38]. Copyright 2021, American Chemical Society.

novel high-performance binders to reduce polymer content. Noteworthy progress has been achieved in the above two aspects in recent years. For instance, Kim *et al.* devised a co-solvent slurry preparation method [33], employing a nonpolar solvent, dibromomethane (DBM), and a polar solvent, hexyl butyrate (HB), to dissolve nitrile-butadiene rubber (NBR) and LiTFSI, and controlled the dispersion degree of binder in the composite process by adjusting the ratio of the two solvents. The NBR chains completely unraveled in a pure DBM solvent, while the NBR chain segments became more aggregated as the proportion of HB increased (Fig. 3a). With an equal ratio of DBM to HB in the solution, the polymer chain segments are highly dispersed at the interface of the composite electrolyte and electrode (Fig. 3b), severely hindering Li^+ transport. Conversely, with a higher proportion of HB in the solution, the influence of NBR on the interface contact is diminished (Fig. 3c).

The electrochemical performances of the SPCSE membranes are significantly influenced by the degree of dispersion, given the limited interactions between components of different polarities in the slurry. Chen *et al.* employed machine learning guidance to evaluate the influence of various manufacturing condition parameters on the SPCSE membranes [38]. They used different Li_6PS_5Cl slurries to fabricate three types of composite membranes with typical characteristics (Fig. 3d). Class 1 represents the most ideal coating state, characterized by uniform application, clear boundaries, and a homogeneous and dense distribution of sulfide solid electrolytes powders. Classes 2 and 3 exhibit varying degrees of draw-

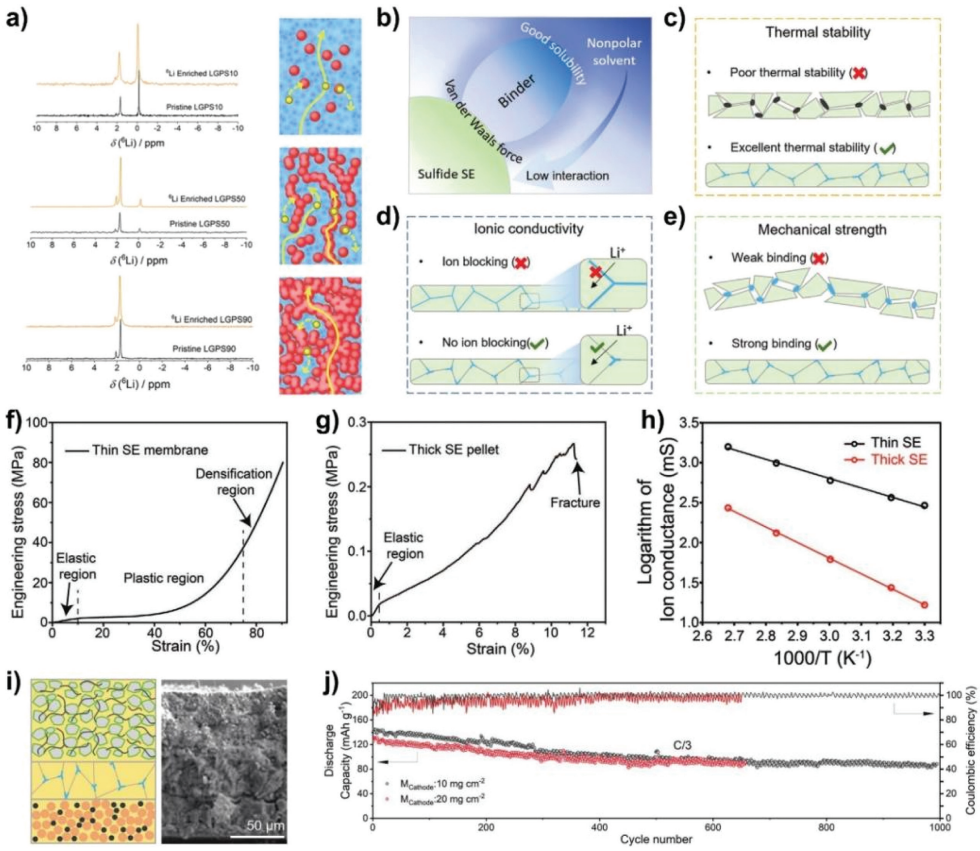

Fig. 4. (a) ^{6}Li MAS NMR spectra before and after cycle ^{6}Li metal electrodes of different composites. Copied with permission [40]. Copyright 2021, American Chemical Society. (b-e) Description of conditions for high efficiency polymer binders. Stress-strain curves of (f) thin SPCSE membrane and (g) thick sulfide solid electrolytes pellet during axial compression. (h) Arrhenius plot of the thin SPCSE membrane and thick solid electrolytes. Copied with permission [41]. Copyright 2021, Wiley. (i) Schematic diagram and SEM image of the whole battery using thin SPCSE membrane. (j) Cyclic properties of cathodes loads of 10 and 20 mg/cm^2, respectively. Copied with permission [42]. Copyright 2022, Wiley.

backs attributable to inappropriate liquid-to-solid ratios. Class 2 exhibits uneven boundaries, whereas Class 3 displays severe aggregation and large cracks as observed in scanning electron microscope (SEM) images. Their work suggests a favorable approach for the future development of scale-up processes for slurry coating method.

Zhang *et al.* systematically explored the impact of toluene, ethyl acetate (EAC) solvents, and polymer electrolytes PVDF and PEO on the microstructure and electrochemical performances of the $78Li_2S$-$22P_2S_5$ (7822 gc)/polymer composite membranes [32]. The addition of lithium salt significantly improved the ion conductivity of the SPCSE membrane. They fabricated a self-supporting 7822 gc SPCSE membrane with a thickness of 120 μm and an ion conductivity ranging from 4 S/cm to 7×10^{-4} S/cm. When paired with a sulfur positive electrode and Li-In negative electrode, the ASSLB exhibited an energy density of 87.0 Ah/L. Their team also employed Li_6PS_5Cl sulfide solid electrolytes characterized by a higher ion conductivity [39]. Employing the same method, they fabricated SPCSE membranes with a thickness ranging of 100–120 μm and an ion conductivity of 1×10^{-3} S/cm. Polarized piezoelectric polymer PVDF filled the gaps between electrolyte powders without impeding lithium-ion transport among Li_6PS_5Cl powders. This method effectively alleviated the growth of lithium dendrites.

Li *et al.* systematically investigated the Li^+ conduction mechanism in SPCSE membranes [40]. They performed ^{6}Li magic angle spinning nuclear magnetic resonance (MAS NMR) spectroscopy on composite materials with LGPS contents at 10%, 50%, and 90% before and after cycling with a ^{6}Li metal electrode. The spectra indicated that Li^+ primarily depends on transport in PEO in composite materials with lower LGPS contents. While in the composite material with 50% LGPS content, Li^+ transport relies on the combined action of sulfide solid electrolytes and the polymer. In composite materials with higher LGPS contents, sulfide solid electrolytes become the primary pathway for Li^+ transport (Fig. 4a).

The introduction of lithium salt has a positive impact on ion conduction, but the predominant factor is still the transport between sulfide solid electrolytes powders. Hence, it is crucial to develop new binders to decrease the polymer content. Efficient polymer binders should satisfy the following criteria: (1) High chemical compatibility with sulfide solid electrolytes and solvents; (2) Excellent thermal stability during high-temperature processes (≈200 °C) for solvent removal; (3) Outstanding mechanical bonding strength; (4) Excellent film-forming properties; and (5) Negligible adverse effects on ion conduction (Figs. 4b-e) [41]. Cao *et al.* utilized the novel binder ethyl cellulose as the polymer binder. This binder is dispersed within the sulfide solid electrolytes membrane rather than forming a continuous coating. The composite membrane (47 μm) prepared through dip-coating displayed a compressive strength of up to 80 MPa during axial compression (Fig. 4f). In contrast, the thick solid electrolytes (976 μm) without a binder experienced fracture at 0.27 MPa (Fig. 4g). The ion conductivity decreased only slightly from 1.67×10^{-3} S/cm to 1.65×10^{-3} S/cm (Fig. 4h), with a retention rate as high as 98.8%. Assembled into an ASSLB, this membrane delivered a high mass energy density of 175Wh/kg and volumetric energy density of 675 Wh/L. In their recent findings, the SPCSE membrane prepared using this process, in combination with a high-capacity NCM811 positive electrode and

Table 1
Parameters of SPCSE membranes prepared by slurry coating method and the resulting ASSLBs in literature.

Sulfide solid electrolytes	Binder	Binder content (wt%)	Solvent	σ_m (mS/cm)	σ_m/σ_p	Thickness (μm)	Cathode/Anode	Energy density	Ref.
$75Li_2S$-$25P_2S_5$	Poly(propylene carbonate)	6	Anisole	0.11	26.8	80	NCM111/Graphite	115 Wh/kg	[36]
$Li_7P_3S_{11}$	SEBS	5	XYL	0.7	58.3	50	—	—	[35]
$78Li_2S$-$22P_2S_5$	PVDF	3	EAC	0.707	39.7	120	S/Li-In	87.0 Ah/L	[32]
$78Li_2S$-$22P_2S_5$	PEO	3	TOL	0.386	21.7	120	S/Li-In	87.0 Ah/L	[32]
Li_6PS_5Cl	PVDF	5–30	EAC	1.21–0.331	<36.2	100–120	—	—	[39]
Li_6PS_5Cl	PEO	5	ACN	0.283	9.4	65	NCM721/Li-In	374.7 W/kg	[31]
Li_6PS_5Cl [a]	Non-aqueous acrylate-type	1	XYL	1.31	72.8	30	NCM90/Ag-C	900 Wh/L	[43]
Li_6PS_5Cl	Ethyl cellulose	2	TOL	1.65	98.8	47	LCO/Li-In	175 Wh/kg 675 Wh/L	[41]
Li_6PS_5Cl	Ethyl ellulose	2	TOL	1.65	98.8	50	NCM811/Si	285 Wh/kg	[42]
$L_{10}GP_2S_{12}$	PEO	90	ACN	0.0122	0.4	—	—	—	[40]
Li_6PS_5Cl	PBMA	3–10	*p*-XYL-IBIB	0.15–0.86	<41.0	40	NCM811/Li-In	—	[38]
$Li_6PS_5Cl_{0.5}Br_{0.5}$ [a]	NBR	5	DBM-HB	—	—	100	NCM70/Graphite	—	[33]
$Li_6PS_5Cl_{0.5}Br_{0.5}$ [a]	NA	3.5	Benzyl acetate	2.2	26.5	8	NCM70/Graphite	—	[44]
$Li_{9.88}GeP_{1.96}Sb_{0.04}S_{11.88}Cl_{0.12}$	P(MMA/nBA)	3	TOL	1.9	27.9	8	LCO/Li	—	[37]
Li_6PS_5Cl	PVDF	2	EAC	—	—	30	LCO/Li-In	—	[45]

[a] This work displayed a soft-pack battery device. SEBS, polystyrene-*block*-polyethylene-*ran*-butylene-*block*-polystyrene; IBIB, isobutyl isobutyrate; NA, nitrile-butadiene rubber–poly(1,4-butylene adipate).

Table 2
Parameters of SPCSE membranes prepared by dry binder laminating method and the resulting ASSLBs in literature.

Sulfide solid electrolytes	Binder	Binder content (wt%)	σ_m (mS/cm)	σ_m/σ_p	Thickness (μm)	Cathode/Anode	Energy density	Ref.
$75Li_2S$-$25P_2S_5$	Polyimine	20	0.1	17.0	64	FeS_2/Li-In	—	[46]
$70Li_2S$-$30P_2S_5$	Aramid fiber	10	2.4	0.6	100	—	—	[47]
$Li_{3.25}Ge_{0.25}P_{0.75}S_4$	PEO	12	0.42	14.9	100	S-PAN/Li	116 Wh/kg 660 Wh/L	[48]
Li_6PS_5Cl [a]	PTFE	0.3	2.7	87	150	NCM90/Graphite	—	[49]
$Li_{5.4}PS_{4.4}Cl_{1.6}$	PTFE	0.2	8.4	77.8	30	NCM523/Li	—	[50]
Li_6PS_5Cl [a]	PTFE	0.5	1.7	70.8	20	LCO/Graphite	—	[51]
Li_6PS_5Cl	PTFE	0.4	1.4	77.8	48	PMTH/Li-In	—	[52]
Li_6PS_5Cl [a]	PTFE	0.2	8.4	94.3	40	NCM622/Li-In	—	[53]
$Li_{10}Si_{0.3}PS_{6.7}Cl_{1.8}$	PTFE	1	1.26	60	130	S/$Li_{3.75}Si$	—	[54]
Li_6PS_5Cl	Polydopamine	—	0.2	5.7	35	Co_3S_4/Li	284.4 Wh/kg	[55]
Li_6PS_5Cl	Polyester fiber	5	2.9	74.4	100	NCM712/Li-In	—	[56]
Li_6PS_5Cl	XNBR	3–10	1	—	47	S/Li	—	[57]
Li_6PS_5Cl	SBR	2	2.34	56.8	80	NCM811/LTO	—	[58]

[a] This work displayed a soft-pack battery device. PMTH, dipentamethylenethiuram hexasulfide; XNBR, carboxylated nitrile-butadiene rubber.

a nano-Si negative electrode (Fig. 4i), exhibited a higher energy density of 285 Wh/kg and excellent cycling performance (Fig. 4j) [42].

Table 1 summarizes recently reported SPCSE membranes using the slurry coating method [31-33,35-45]. Despite the numerous advantages of the wet compositing process, the used solvents inevitably reduce the ionic conductivity, and the environmental impact of solvent is not in line with the principles of sustainable development. Therefore, further research and exploration are required for the wet processing of SPCSE membranes.

3.2. Dry binder laminating method

To fundamentally address the adverse impacts resulting from solvents use in wet processes, researchers have proposed a solvent-free dry process as an alternative (Table 2) [46-58]. In this process, sulfide solid electrolytes powders and polymer binders are thoroughly mixed, and the binder is subsequently formed into a continuous cross-linked network between powders through pressing or rolling. Because the dry binders used in this process usually exhibit thermoplastic properties, suitable heating during processing assists in the dispersion of the binder among the sulfide solid electrolytes powders. As illustrated in Fig. 5a, Lee *et al.* employed hot isostatic pressing at 100 °C and 280 MPa to fill the gaps in sulfide solid electrolytes with polyimide [46], creating an *in-situ* cross-linked polymer mechanism that does not fully disturb the contact between individual powders. They fabricated a SPCSE membrane with a thickness of around 100 μm and an 80% sulfide solid electrolytes content. In a similar fashion, Yersak *et al.* utilized hot pressing at 240 °C and 200 MPa to incorporate 10 wt% aramid fibers and $70Li_2S$-$30P_2S_5$ sulfide glass-ceramic solid electrolytes, displaying a thickness of 100 μm and an ion conductivity of 2.4×10^{-3} S/cm [47]. Likewise, Li *et al.* blended LGPS, LiTFSI, and PEO plasticized with Pyr1,4TFSI, preparing a SPCSE membrane through hot pressing with a thickness of 100 μm (Fig. 5b) [48]. The battery assembled with this membrane, coupled with the S/polyacrylonitrile (PAN) cathode, displayed exceptional cycling and rate performances.

In 2019, Hippouf and colleagues proposed a dry membrane process employing only 0.3 wt% PTFE as a binder [49]. They efficiently fabricated a flexible SPCSE membrane, 150 μm in thickness, with an ion conductivity of 2.7×10^{-3} S/cm by using a straightforward cold pressing technique. Owing to the fibrous nature of PTFE, it minimizes surface contact between the active material and the binder molecules. Due to its exceptional binding properties, PTFE enables the reduction of binder content (< 1 wt%) in the dry process, establishing it as the most prevalent binder in dry processes. Fig. 5c depicts the typical preparation process [50]. Zhang *et al.* employed highly conductive $Li_{5.4}PS_{4.4}Cl_{1.6}$ sulfide solid electrolytes powders and 0.2 wt% PTFE as raw materials. They used the shear force generated by mechanical ball milling to transform PTFE into fibrous form. Finally, a SPCSE membrane with the desired thickness was obtained through hot pressing with roll-to-roll at 80 °C. Nano-sized PTFE fibers are visible in SEM images (Fig. 5d). Through process

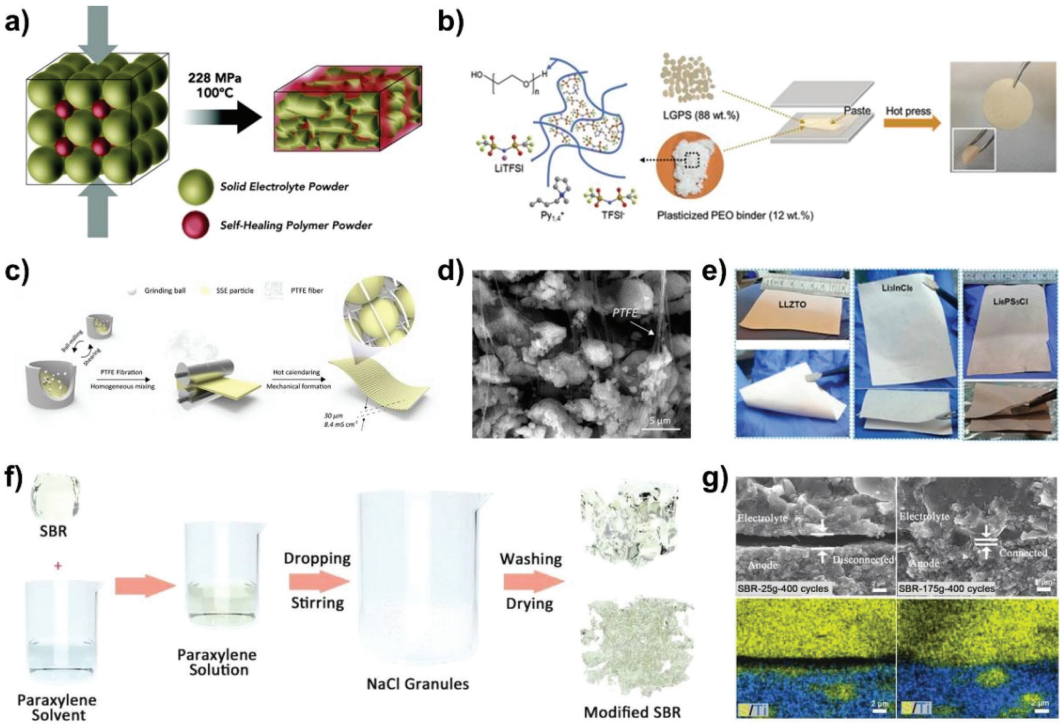

Fig. 5. (a) Dry binder laminating method of Li_2S-P_2S_5/polyimine SPCSE membrane by hot pressing. Copied with permission [46]. Copyright 2015, Wiley. (b) Preparation diagram of LGPS/PEO SPCSE membrane. Copied with permission [48]. Copyright 2019, Wiley. (c) Roller pressing for $Li_{5.4}PS_{4.4}Cl_{1.6}$/PTFE SPCSE membrane. (d) SEM image of nanofibrous PTFE after rolling. Copied with permission [50]. Copyright 2021, American Chemical Society. (e) Optical photos of composite membranes prepared by PTFE and different types of solid electrolytes. Copied with permission [51]. Copyright 2021, American Chemical Society. (f) SBR topography optimization diagram. (g) SEM and EDS images of interfaces between electrodes and electrolytes after 400 cycles of the whole battery prepared with binders of different optimization degrees. Copied with permission [58]. Copyright 2022, Wiley.

optimization, they achieved a reduced thickness (30 μm) and the highest reported ion conductivity to date (8.4×10^{-3} S/cm). Fig. 5e shows large-area composite membranes prepared with PTFE and various types of solid electrolytes, further emphasizing the feasibility of this process [51].

Nevertheless, PTFE might not be the optimal choice as a polymer binder. *Via* electrochemical reduction, PTFE within the SPCSE membrane undergoes defluorination and reacts with lithium metal on the negative electrode side, ultimately producing conductive sp^2 carbon [59]. This disrupts the passivating SEI layer and enhances the electronic conductivity of the sulfide solid electrolytes, so the modification of the Li-electrolyte interface is essential during the assembly of ASSLBs. Hence, there is an urgent need for a dry binder with higher chemical stability to Li to replace PTFE. Lee *et al*. employed polyester fibers with a weight percentage of 5% [56], thermally pressed alongside Li_6PS_5Cl, to fabricate a self-supporting SPCSE membrane with a thickness of 100 μm. The membrane exhibited an ion conductivity of 2.9×10^{-3} S/cm at room temperature. The polyester fibers contributed to both robust mechanical strength and thermal stability. The researchers reported consistent deposition and stripping behavior in lithium symmetric cells, highlighting remarkable interface stability with lithium.

Styrene-butadiene rubber (SBR), the predominant binder for graphite cathode in lithium-ion batteries, possesses a higher highest occupied molecular orbital (HOMO) level than PVDF, suggesting reduced susceptibility to reduction on the lithium metal side. Leveraging its outstanding interface stability with lithium, Li *et al.* systematically developed and optimized SBR to augment its dispersibility and mechanical stretchability in dry processes [58]. The optimized procedure is illustrated in Fig. 5f. The original SBR was dissolved in xylene and then precipitated onto various quantities of NaCl templates, allowing for the adjustment of the binder's size and microstructure. Throughout the precipitation process, xylene was adsorbed by NaCl, leading to the separation of the binder from the surface of NaCl powders. As a base, NaCl could be easily removed. The researchers crafted SPCSE membranes using SBR with identical mass but varying specific surface areas, revealing notable performance distinctions. Enhanced dispersion resulted in decreased electrochemical impedance of the SPCSE membrane, accompanied by a gradual increase in ion conductivity. The modified membrane displayed the highest ion conductivity, reaching 2.34×10^{-3} S/cm, a significant improvement over the unmodified counterpart (1.29×10^{-3} S/cm). This enhancement arises from the lower hardness and Young's modulus of the internally porous and loose binder formed during precipitation. Under identical mass conditions, the modified SBR exhibits a larger volume and specific surface area, effectively mitigating processing challenges in the dry process and reducing polymer aggregation in the SPCSE membranes. The same binder is also employed in electrode manufacturing. The SEM images of the electrode-electrolyte interface revealed a tight connection of the interface of the electrode consisting of the modified SBR-175 g with a larger specific surface area while significant cracks with a smaller specific surface area SBR-25g (Fig. 5g). This resulted in a decline in the cyclic performance of the battery, which further underscoring the importance of binder modification. Their work provides a new idea for the design of high-performance binders in dry binder laminating method.

3.3. Skeleton templating method

While the above two methods have succeeded in reducing the thickness of sulfide solid electrolytes membrane to some extent, the inadequate effective adhesion resulting from the lower binder content still poses significant challenges in assembling pouch cells

Table 3
Parameters of SPCSE membranes prepared by skeleton templating method and the resulting ASSLBs in literature.

Sulfide solid electrolytes	Template	Template content (wt%)	Binder	Solvent	σ_m (mS/cm)	σ_m/σ_p	Thickness (μm)	Cathode/Anode	Energy density (Wh/kg)	Ref.
Li_3PS_4[a]	PPTA NW	14	—	TOL	0.2	27.4	70	LCO/LTO	44	[60]
Li_3PS_4	Kevlar NW	—	—	TOL	0.3	53.6	100	Li_2S/Li	370.6	[62]
$Li_6PS_5Cl_{0.5}Br_{0.5}$[a]	PI	3.6–6.6	—	EtOH	0.058	2.9	40–70	NCM622/Graphite	110	[61]
Li_6PS_5Cl[a]	Cellulose	—	Silicone rubber	Chloroform	6.3	73.2	60	S/Li-In	—	[63]
$L_{10}GP_2S_{12}$	Nylon	—	PTFE	—	0.36	9.2	100	NCM532/Li	—	[64]
$L_{10}GP_2S_{12}$[a]	Nylon	22.5	PEO	Anisole	0.24	6.1	60	NCM622/Li	—	[65]
Li_6PS_5Cl[a]	P(VDF-TrFE)	21	—	TOL	1.2	30.8	40	NCM811/Li-In	—	[66]
Li_6PS_5Cl	PE	—	NBR	XYL	0.51	16.1	45	NCM70/Li	314.3	[67]
$Li_{5.7}PS_{4.7}Cl_{1.3}$[a]	Poly(ethylene vinyl acetate)	7.5	PTFE	—	1.1	13.6	40	NCM811/Li	354.4	[68]

[a] This work displayed a soft-pack battery device.

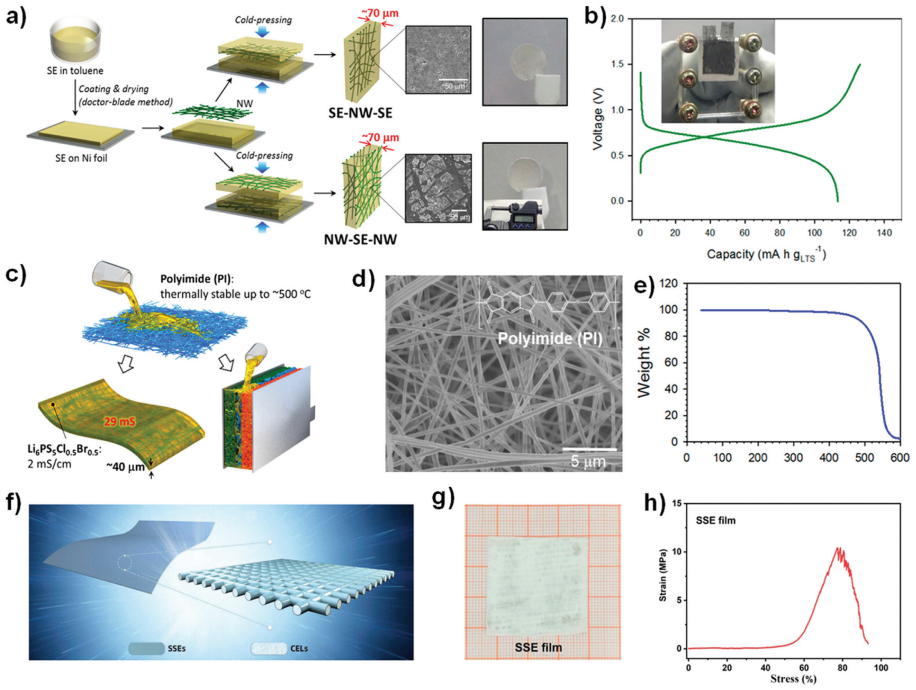

Fig. 6. (a) Schematic diagram of preparation of two NW-electrolyte membranes with different structures. (b) The first charge and discharge curves of the lamella LTS/LTO full battery with SPCSE membrane at 89 μA/cm^2 at 30 °C. Copied with permission [60]. Copyright 2015, American Chemical Society. (c) Flow chart of preparation of SPCSE membrane by electrospinning porous PI NWs permeated by ethanol solution of $Li_6PS_5Cl_{0.5}Br_{0.5}$. (d) SEM image of porous PI NWs by electrospinning. (e) TGA atlas of PI NWs in Ar atmosphere. Copied with permission [61]. Copyright 2020, American Chemical Society. (f) Schematic diagram of a flexible SPCSE membrane with a crossed CELs skeleton. (g) Optical photographs of a flexible SPCSE membrane with CELs skeleton. (h) The stress-strain curves of the SPCSE membrane. Copied with permission [63]. Copyright 2021, Wiley.

with high-volume deformation electrodes. In response to this issue, some researchers advocate the skeleton templating method as a solution. The recent results are summarized in Table 3 [60-68]. In this approach, sulfide solid electrolytes powders infiltrate and fill into a porous support framework to establish an ion transport pathway, which a continuous cross-linked framework enhances both the mechanical strength and processability of the SPCSE membrane. For example, Nam *et al.* detailed the production of a flexible SPCSE membrane, in which employs poly(paraphenylene terephthalamide) nonwoven (PPTA NW) as the structural base [60]. The manufacturing process is depicted in Fig. 6a. A TOL solution of sulfide solid electrolytes was cast onto a Ni foil substrate and subsequently dried. The dried solid electrolytes were cold-pressing with the nonwoven (NW) framework, yielding two distinct structured SPCSE membranes (electrolyte-NW-electrolyte and NW-electrolyte-NW). Both membranes displayed a thickness of approximately 70 μm, accompanied by an ionic conductivity exceeding 0.16 mS/cm. The assembled sheet battery $LiTiS_2$/electrolyte-NW-electrolyte/$Li_4Ti_5O_{12}$ exhibited an outstanding reversible capacity during the initial cycle (Fig. 6b). Kim *et al.* proposed a new large-scale manufacturing scheme for ASSLBs [61]. Specifically, the procedure involves injecting an ethanol solution of $Li_6PS_5Cl_{0.5}Br_{0.5}$ into a pre-assembled pouch-type cathode/polymer NW membrane/anode, followed by evaporating the solvent and recrystallizing the sulfide solid electrolytes at high temperature. The same approach is applied to produce flexible SPCSE membranes, as illustrated in Fig. 6c. The team opted for a polyimide (PI) electrospun membrane, characterized by excellent porosity (Fig. 6d) that facilitates solution penetration. The thermal stability of this membrane (nearing 500 °C) surpasses the recrystallization temperature of $Li_6PS_5Cl_{0.5}B_{r0.5}$ (400 °C), ensuring favorable ionic conductivity post-sulfide solid electrolytes recrystallization (Fig. 6e). The assembled NCM/PI-$Li_6PS_5Cl_{0.5}Br_{0.5}$/Gr ASSLB attains an energy density of 110 Wh/kg.

It is essential to consider the following factors when choosing a support framework: (1) Larger porosity and appropriate pore size

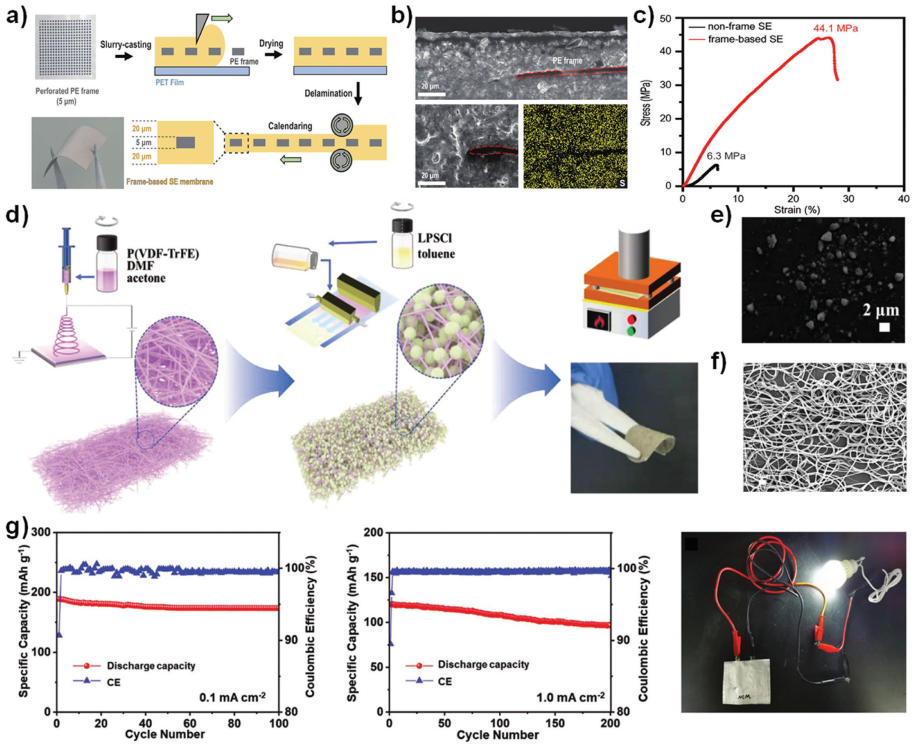

Fig. 7. (a) Preparation process diagram of Li_6PS_5Cl SPCSE membranes supported by porous PE frame. (b) SEM and EDS images of SPCSE membranes. (c) Comparison diagram of stress-strain curves of frame-based SPCSE membrane and non-frame SPCSE membrane. Copied with permission [67]. Copyright 2023, Wiley. (d) Flow chart of preparation of SPCSE membrane by electrospinning P(VDF-TrFE) membrane permeated by the toluene solution of Li_6PS_5Cl. SEM images of (e) Li_6PS_5Cl powders and (f) electrospinning P(VDF-TrFE). (g) The cycle performance diagram of pouch type cells at different current densities and capable of powering a light bulb. Copied with permission [66]. Copyright 2022, Wiley.

to facilitate ample penetration of sulfide solid electrolytes powders. (2) Optimal thickness. (3) Good mechanical strength and flexibility. (4) High thermal stability, allowing for high-temperature processing. Additionally, when opting for a support framework with large pores, it is imperative to employ a binder for ensuring the effective binding of sulfide solid electrolytes powders within these pores. For instance, Zhu *et al.* employed 1% silicon rubber as a binder and cellulose film (CEL) as the support framework to fabricate a Li_6PS_5Cl SPCSE membrane with a thickness of 60 μm (Fig. 6f) [63]. Fig. 6g presents the optical photograph of the SPCSE membrane. The thickness of the composite membrane was solely determined by the thickness of CEL films, due to the interaction between CEL fibers and solid electrolytes. The continuous and intact fiber network significantly enhances the mechanical strength of the composite SE membrane, as evidenced by a tensile strength of up to 10.4 MPa in tensile tests (Fig. 6h). Liang's group utilized PEO as a binder and a nylon mesh as a reinforcing network to produce an ultra-thin (60 μm) LGPS SPCSE membrane with high mechanical strength (13.8 MPa) [65]. The identical nylon-reinforced network was employed by the team for manufacturing dry composite membranes [64]. Initially, a SPCSE membrane was created using PTFE as a binder. Subsequently, reinforcement was accomplished by straightforward roll pressing on both sides of the PTFE film with the nylon network.

In a recent study, Kim *et al.* devised a SPCSE membrane utilizing NBR as binders and perforated commercial polyethylene (PE) as a reinforcing framework (Fig. 7a) [67]. The 35% porosity of the framework with 1 mm aperture ensures ample penetration of sulfide solid electrolytes. Cross-sectional SEM illustrates the close dispersion of sulfide solid electrolytes on both sides of the approximately 5 μm thick PE membrane, forming a continuous Li^+ pathway (Fig. 7b). The PE-reinforced framework significantly enhances the tensile strength of the composite membrane, reaching 44.1 MPa, which is seven times higher than that of the non-framework structure (Fig. 7c).

Liu *et al.* fabricated a SPCSE membrane composed of poly(vinylidene fluoride-*co*-trifluoroethylene) (PVDF-TrFE) flexible framework and Li_6PS_5Cl by electrospinning and hot-press infiltration (Fig. 7d) [66]. The sulfide solid electrolytes powders with a diameter of approximately 1–3 μm were obtained through grinding and sieving (Fig. 7e). The SEM image of the electrospun polymer framework distinctly revealed a network structure with a diameter greater than that of the sulfide solid electrolytes powders. These sizable voids played a crucial role in facilitating the penetration treatment with the sulfide-toluene solution (Fig. 7f). Following permeation drying, two composite membranes were stacked and hot-pressed at 200 °C and 10 MPa for 2 h. At high temperatures, thermoplastic PVDF-TrFE permeates evenly throughout the SPCSE membrane, playing a bonding role and reducing the use of additional polymer binders. A coin-type cell, comprising a SPCSE membrane, NCM811 cathode, and Li-In anode, exhibited the remarkably prolonged cycling performance, with a capacity retention of 71% after 20,000 cycles at 1.0 mA/cm^2 (1.16 C). Pouch-type cells, featuring the same electrolyte and electrodes, showcased the similar high capacity and retention rates both at 0.1 mA/cm^2 and 1.0 mA/cm^2, powering LED bulbs (Fig. 7g).

4. Conclusions and perspectives

In summary, the design of SPCSE membranes by introducing polymers as binder or supporting architecture into sulfide electrolytes emerges as an effective strategy to enhance mechanical properties of sulfide electrolytes. This review outlines the latest advancements in designing and preparing thin SPCSE membranes, systematically discussing the challenges and solutions encountered by different designing strategies. In the future, further efforts are

imperative to improve the performance of SPCSE membranes, including achieving better mechanical strength (thus enabling much thinner SPCSE membranes) and utilizing simpler preparation process based on customized material systems (Fig. 8), for accelerating the large-scale application of high energy density ASSLBs with sulfide electrolytes. The potential developments about design and preparation of SPCSE membranes are proposed as follows:

(1) Tailoring matched solvent-binder systems for slurry coating method. Currently, due to challenges with binder dispersion and sulfide self-decomposition in traditional electrolyte composite slurries, non-polar solvent-binder systems like PVDF-EAC and PEO-ACN have been proposed in some literatures. Additionally, strategies, involving dual solvents to regulate binder morphology and sulfide electrolyte doping engineering to enhance solvent tolerance, have been documented. However, several issues persist, including insufficient binder dispersion and low retention about ion conductivities of sulfide solid electrolytes. Moving forward, it is crucial to strike a balance between binder adhesion, solvent solubility, and sulfide solid electrolytes ion conductivity to further reduce polymer binder content and enhance composite membrane performance (Fig. 8a).

(2) Developing dry binders with high adhesive strength and specific surface for rolling and pressing. Although the dry process avoids the use of solvents, large-scale production and application of roller press equipment require higher standards for working pressure, uniformity, and roll precision. Currently, the selection of binders for the dry method is limited, with the use of PTFE-based binders restricted by their poor stability with the negative side and Li metal. Other binders face challenges of insufficient bonding and poor dispersion when content is reduced further. In the future, the specific surface area of the binders typically used in the existing dry process should be maximized (Fig. 8b), thereby reducing the processing difficulty of the dry process, and more efficient types of dry binders are expected to be designed with advanced chemical and molecular engineering techniques.

(3) Further improving the mechanical strength. Compared to liquid commercial separators, SPCSE membranes are generally thicker, and the assembled ASSLBs's energy density is still not as high as expected; Further reducing their thickness requires a more solid SPCSE membrane. Currently, only a few studies characterize the mechanical strength of SPCSE membranes through stress and strain tests. While enhancing the support skeleton effectively improves the mechanical strength of the SPCSE membrane, the insulating skeleton hinders the transport of lithium ions, resulting in a low conductivity of the skeleton supported SPCSE membrane. In the future, high-energy-density ASSLBs with high capacity and large-volume deformation electrodes, will require higher mechanical properties of SPCSE membranes (Fig. 8c). The better supporting skeleton structure and functional sulfide electrolyte filler show huge research prospects, and a unified quantitative standard for evaluating the mechanical strength of SPCSE membranes is also needed.

(4) Designing elaborate interface structures between electrode and electrolyte for intimate contact. Less than half of the current studies have reported on fabricating pouch batteries device with SPCSE membranes. The limited pressure in pouch batteries leads to contact loss at the 2D solid-solid interface between the electrode and the SPCSE membrane during cycling, affecting the lifespan of the batteries. Further design of a rational electrode-SPCSE membrane interface structure is necessary. For instance, with 3D printing technology, the composite electrolytes slurry can be precisely cast onto pre-prepared 3D electrode area (Fig. 8d), then the slurry can fully infiltrate the 3D electrode, forming a three-dimensional electrode-electrolyte membrane contact. An efficient three-dimensional contact interface creates an all-in-one electrode-electrolyte membrane structure, effectively resolving interfacial contact loss. On the other hand, this structure demonstrates higher integrity, which can prevent short circuits in the battery caused by damage to SPCSE membranes, thereby further reducing the use of the electrolyte layer.

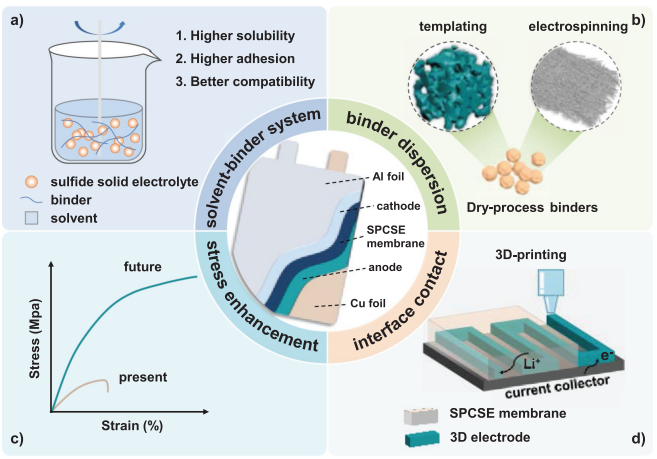

Fig. 8. (a-d) Schematic diagram of design strategy of SPCSE membranes for the development and realization of high performance and high energy density sulfide ASSLBs.

Declaration of competing interest

The authors declare that they have no known competing financial interests or personal relationships that could have appeared to influence the work reported in this paper.

CRediT authorship contribution statement

Xingjie Li: Writing – original draft. **Chengjun Yi:** Writing – original draft. **Weifei Hu:** Writing – review & editing. **Huishan Zhang:** Writing – review & editing. **Jiale Xia:** Writing – review & editing. **Yuanyuan Li:** Writing – review & editing. **Jinping Liu:** Writing – review & editing.

Acknowledgments

This work was supported by grants from the National Natural Science Foundation of China (Nos. 52072136, 52172229, 52272201, 52302303, 51972257), Yanchang Petroleum-WHUT Joint Program (No. yc-whlg-2022ky-05) and Fundamental Research Funds for the Central Universities (Nos. 104972024RSCrc0006, 2023IVA106) for financial support.

References

[1] D.H. Tan, A. Banerjee, Z. Chen, et al., Nat. Nanotechnol. 15 (2020) 170–180.
[2] A. Manthiram, X. Yu, S. Wang, Nat. Rev. Mater. 2 (2017) 1–16.
[3] C. Yi, W. Liu, L. Li, et al., Funct. Mater. Lett. 12 (2019) 1930006.
[4] W. Liu, C. Yi, L. Li, et al., Angew. Chem. 133 (2021) 13041–13050.
[5] K.J. Kim, M. Balaish, M. Wadaguchi, et al., Adv. Energy Mater. 11 (2021) 2002689.
[6] Q. Song, Y. Zhang, J. Liang, et al., Chin. Chem. Lett. 35 (2024) 108797.
[7] T. Ma, Z. Wang, D. Wu, et al., Energy Environ. Sci. 16 (2023) 2142–2152.
[8] Z. Wang, Z. Mu, T. Ma, et al., Adv. Mater. 36 (2024) 2310395.
[9] H. Zhang, Z. Yu, J. Cheng, et al., Chin. Chem. Lett. 34 (2023) 108228.
[10] M. Kammoun, S. Berg, H. Ardebili, Nanoscale 7 (2015) 17516–17522.

[11] D. Li, L. Chen, T. Wang, et al., ACS Appl. Mater. Interfaces 10 (2018) 7069–7078.
[12] H. Xiang, N. Deng, L. Gao, et al., Chin. Chem. Lett. 35 (2024) 109182.
[13] Y. Ren, K. Chen, R. Chen, et al., J. Am. Ceram. Soc. 98 (2015) 3603–3623.
[14] D.H. Tan, Y.T. Chen, H. Yang, et al., Science 373 (2021) 1494–1499.
[15] Z. Liang, Y. Xiao, K. Wang, et al., Energy Storage Mater. 63 (2023) 102987.
[16] Y. Nomura, K. Yamamoto, Adv. Energy Mater. 13 (2023) 2203883.
[17] C.T. Love, J. Power Sources 196 (2011) 2905–2912.
[18] E. Wang, C.H. Chiu, P.H. Chou, J. Power Sources 461 (2020) 228148.
[19] H. Pan, M. Zhang, Z. Cheng, et al., Sci. Adv. 8 (2022) eabn4372.
[20] T.A. Yersak, J. Shin, Z. Wang, et al., ECS Electrochem. Lett. 4 (2015) A33.
[21] L. Ming, D. Liu, Q. Luo, et al., Chin. Chem. Lett. 35 (2024) 109387.
[22] A. Sakuda, A. Hayashi, T. Ohtomo, et al., J. Power Sources 196 (2011) 6735–6741.
[23] M. Ogawa, R. Kanda, K. Yoshida, et al., J. Power Sources 205 (2012) 487–490.
[24] H. Liu, Y. Liang, C. Wang, et al., Adv. Mater. 35 (2023) 2206013.
[25] Y. Liu, T. Yu, S. Guo, et al., Acta Phys. Chim. Sin. 39 (2023) 2301027.
[26] H. Jiangkui, Y. Hong, Z. Chenzi, et al., J. Chin. Ceram. Soc. 50 (2022) 110–120.
[27] C. Wang, J. Liang, Y. Zhao, et al., Energy Environ. Sci. 14 (2021) 2577–2619.
[28] Y. Kato, S. Hori, T. Saito, et al., Nat. Energy 1 (2016) 1–7.
[29] J. Xu, Y. Li, P. Lu, et al., Adv. Energy Mater. 12 (2022) 2102348.
[30] T. Yersak, J.R. Salvador, R.D. Schmidt, et al., Int. J. Appl. Glass Sci. 12 (2021) 124–134.
[31] S. Luo, Z. Wang, A. Fan, et al., J. Power Sources 485 (2021) 229325.
[32] Y. Zhang, R. Chen, S. Wang, et al., Energy Storage Mater. 25 (2020) 145–153.
[33] K.T. Kim, D.Y. Oh, S. Jun, et al., Adv. Energy Mater. 11 (2021) 2003766.
[34] Y. Nikodimos, C.J. Huang, B.W. Taklu, et al., Energy Environ. Sci. 15 (2022) 991–1033.
[35] D.H. Tan, A. Banerjee, Z. Deng, et al., ACS Appl. Energy Mater. 2 (2019) 6542–6550.
[36] M. Yamamoto, Y. Terauchi, A. Sakuda, et al., Sci. Rep. 8 (2018) 1212.
[37] X. Zhao, P. Xiang, J. Wu, et al., Nano Lett. 23 (2022) 227–234.
[38] Y.T. Chen, M. Duquesnoy, D.H. Tan, et al., ACS Energy Lett. 6 (2021) 1639–1648.
[39] S. Wang, X. Zhang, S. Liu, et al., J. Materiomics 6 (2020) 70–76.
[40] M. Li, M. Kolek, J.E. Frerichs, et al., ACS Sustain. Chem. Eng. 9 (2021) 11314–11322.
[41] D. Cao, Q. Li, X. Sun, et al., Adv. Mater. 33 (2021) 2105505.
[42] D. Cao, X. Sun, Y. Li, et al., Adv. Mater. 34 (2022) 2200401.
[43] Y.G. Lee, S. Fujiki, C. Jung, et al., Nat. Energy 5 (2020) 299–308.
[44] D.Y. Oh, K.T. Kim, S.H. Jung, et al., Mater. Today 53 (2022) 7–15.
[45] Y. Kim, C. Juarez-Yescas, D.W. Liao, et al., ACS Energy Lett. 9 (2024) 1353–1360.
[46] J.M. Whiteley, P. Taynton, W. Zhang, et al., Adv. Mater. 27 (2015) 6922–6927.
[47] T. Yersak, J.R. Salvador, R.D. Schmidt, et al., ACS Appl. Energy Mater. 2 (2019) 3523–3531.
[48] M. Li, J.E. Frerichs, M. Kolek, et al., Adv. Funct. Mater. 30 (2020) 1910123.
[49] F. Hippauf, B. Schumm, S. Doerfler, et al., Energy Storage Mater. 21 (2019) 390–398.
[50] Z. Zhang, L. Wu, D. Zhou, et al., Nano Lett. 21 (2021) 5233–5239.
[51] C. Wang, R. Yu, H. Duan, et al., ACS Energy Lett. 7 (2021) 410–416.
[52] W. Ji, X. Zhang, D. Zheng, et al., Adv. Funct. Mater. 32 (2022) 2202919.
[53] J. Li, Y. Li, S. Zhang, et al., Chem. Eng. J. 455 (2023) 140605.
[54] Z. Lv, J. Liu, C. Li, et al., eTransportation 19 (2024) 100298.
[55] G. Liu, J. Shi, M. Zhu, et al., Energy Storage Mater. 38 (2021) 249–254.
[56] S.E. Lee, H.T. Sim, Y.J. Lee, et al., J. Power Sources 542 (2022) 231777.
[57] S. Kim, Y.A. Chart, S. Narayanan, et al., Nano Lett. 22 (2022) 10176–10183.
[58] Y. Li, Y. Wu, T. Ma, et al., Adv. Energy Mater. 12 (2022) 2201732.
[59] L. Kavan, Chem. Rev. 97 (1997) 3061–3082.
[60] Y.J. Nam, S.J. Cho, D.Y. Oh, et al., Nano Lett. 15 (2015) 3317–3323.
[61] D.H. Kim, Y.H. Lee, Y.B. Song, et al., ACS Energy Lett. 5 (2020) 718–727.
[62] R. Xu, J. Yue, S. Liu, et al., ACS Energy Lett. 4 (2019) 1073–1079.
[63] G.L. Zhu, C.Z. Zhao, H.J. Peng, et al., Adv. Funct. Mater. 31 (2021) 2101985.
[64] T. Jiang, P. He, Y. Liang, et al., Chem. Eng. J. 421 (2021) 129965.
[65] H. Liu, P. He, G. Wang, et al., Chem. Eng. J. 430 (2022) 132991.
[66] S. Liu, L. Zhou, J. Han, et al., Adv. Energy Mater. 12 (2022) 2200660.
[67] D. Kim, H. Lee, Y. Roh, et al., Adv. Energy Mater. 14 (2024) 2302596.
[68] D. Li, H. Liu, C. Wang, et al., Adv. Funct. Mater. 34 (2024) 2315555.